A COMPARISON OF FINITE ELEMENT AND FOURIER SERIES SOLUTIONS AS APPLIED TO RADIALLY LOADED CIRCULAR RINGS

by

Owen Charles Baker

UNITED STATES
NAVAL POSTGRADUATE SCHOOL

THESIS

A COMPARISON OF FINITE ELEMENT
AND FOURIER SERIES SOLUTIONS AS
APPLIED TO RADIALLY LOADED CIRCULAR RINGS

by

Owen Charles Baker

June, 1968

A COMPARISON OF FINITE ELEMENT AND FOURIER SERIES SOLUTIONS AS APPLIED TO RADIALLY LOADED CIRCULAR RINGS

by

Owen Charles Baker
Major, United States Marine Corps
B.S., United States Naval Academy, 1957

Submitted in partial fulfillment of the
requirements for the degree of

MASTER OF SCIENCE IN AERONAUTICAL ENGINEERING

from the

NAVAL POSTGRADUATE SCHOOL
June 1968

ABSTRACT

An examination and a comparison of the relative merits of the finite element and Fourier series methods of solving radially loaded circular ring problems are made. The procedure employed to evaluate the two methods is to use each method to solve for three different load conditions and to compare the performance of the two methods on the basis of accuracy, ease of usage, and equipment required. The results indicate a satisfactory accuracy for both methods under most conditions. The Fourier series method is superior for solving problems with a distributed load condition. The finite element method is superior for solving problems with concentrated loads.

TABLE OF CONTENTS

LIST OF TABLES

LIST OF FIGURES

TABLE OF SYMBOLS

a	Radius of ring, measured from ring axis to middle surface, inches
b	Width of ring, measured parallel to ring axis, inches
k	Abbreviation for $t^2/12a^2$, dimensionless
m	Fourier series mode number, non-dimensional
t	Thickness of ring, measured in radial direction, inches
$\{u\}$	Column matrix of displacement, inches
v	Tangential displacement, inches
v_m	Fourier series coefficient for tangential displacement, inches
w	Radial displacement, inches
w_m	Fourier series coefficient for radial displacement, inches
$\bar{w}$	Non-dimensional radial displacement, wEI/a^3P
z	Distance from middle surface, positive in outward radial direction, inches
A	Ring cross sectional area, $A = bt$, square inches
D	Extensional rigidity, Et, pounds per inch
E	Modulus of elasticity, pounds per square inch
I	Ring cross-sectional area moment of inertia, $bt^3/12$, inches to the fourth
K	Flexural rigidity, $Et^3/12$, inch-pounds
$[K]$	Assembled structure stiffness matrix, pounds per inch
$[K_\eta]$	Element stiffness matrix, pounds per inch
$[K_\rho]$	Reduced assembled structure stiffness matrix, pounds per inch
M	Bending moment in finite element analysis, inch-pounds

M^o	Initial bending moment in finite element analysis, inch-pounds
M_ϕ	Bending moment in Fourier series analysis, pounds
$\bar{M}_\phi$	Non-dimensional bending moment, bM_ϕ/aP
N	Normal force in finite element analysis, pounds
N^o	Initial normal force in finite element analysis, pounds
N_ϕ	Normal force in Fourier series analysis, pounds per inch
$\bar{N}_\phi$	Non-dimensional normal force, bN_ϕ/P
P	Inward radial load applied on both sides of plane $\phi = \pm \pi/2$, pounds
P_r	Applied radial load, positive in outward radial direction, pounds per square inch
P_m	Fourier series coefficient for applied radial load, pounds per square inch
Q	Radial shear force in finite element analysis, pounds
Q^o	Initial radial shear force in finite element analysis, pounds
Q_ϕ	Radial shear force in Fourier series analysis, pounds per inch
U_a	Axial strain energy, inch-pounds
U_b	Bending strain energy, inch-pounds
U_t	Total strain energy, axial plus bending, inch-pounds
$\{X\}$	Assembled structure nodal forces, pounds
$\{X^o\}$	Assembled structure initial forces, pounds
$\{X_\eta\}$	Element nodal forces, pounds
$\{X^o_\eta\}$	Element initial forces, pounds
$\{X_\rho\}$	Reduced assembled structure nodal forces, pounds
$\{X^o_\rho\}$	Reduced assembled structure initial forces, pounds

α	Central half angle, degrees or radians
β	Central angle, degrees or radians
ε_ϕ	Circumferential strain, inches per inch
ϕ	Ring generator angle, degrees or radians
σ_ϕ	Circumferential stress, pounds per square inch
θ	Node rotation in finite element analysis; radians
$[\ ]$	Square matrix
$\{\ \}$	Column matrix

CHAPTER I

INTRODUCTION

The structural analysis of many aerospace vehicles, such as rockets, re-entry bodies, aircraft, space capsules, etc., is frequently accomplished using either the Fourier series method or the finite element method in conjunction with a digital computer. A considerable amount of effort has been devoted to the development and refinement of these two methods, but little attention has been given to a direct comparison of the methods. Fundamental questions regarding the similarities, differences, relative accuracy, ease of usage, and advantages or disadvantages of each of the methods have not been answered as yet. The objective of this study was to seek answers to some of these fundamental questions.

The procedure employed to accomplish the objective was to apply the two methods of analysis to a portion of a typical aerospace structure and to investigate the relative merits of the two methods. The portion selected for analysis was a thin circular ring with a rectangular cross section. The ring was selected because it represents, in a simplified manner, the circular cylinders that are frequently found in aerospace vehicles. Three different load conditions were applied to the ring for each of the two methods of analysis so that the effects of the load distributions on the performance of the two methods could be investigated. The extent to which the analyses were carried out in

terms of numbers of significant figures carried, numbers of terms evaluated in the Fourier series method, number of elements used, and use of double precision techniques in the FORTRAN computer programs, was greater than that normally used in common engineering practice. The reason for such depth was to bring out any subtleties peculiar to either of the two methods that might not appear if normal engineering accuracy were used.

The author gratefully acknowledges the guidance and assistance of Professor Robert E. Ball in the preparation of this thesis.

CHAPTER II

DERIVATION OF THE GOVERNING EQUATIONS FOR THE FOURIER SERIES ANALYSIS

Consider the thin ring shown in Figure 1 where a is the radius of the ring middle surface; b, the ring width; and t, the thickness. The angle ϕ is the generator of the ring and is positive in a counter clockwise direction. All points in the ring are located by the coordinates ϕ and z, where z originates at the middle surface and is positive in the outward radial direction. The normal force N_ϕ,

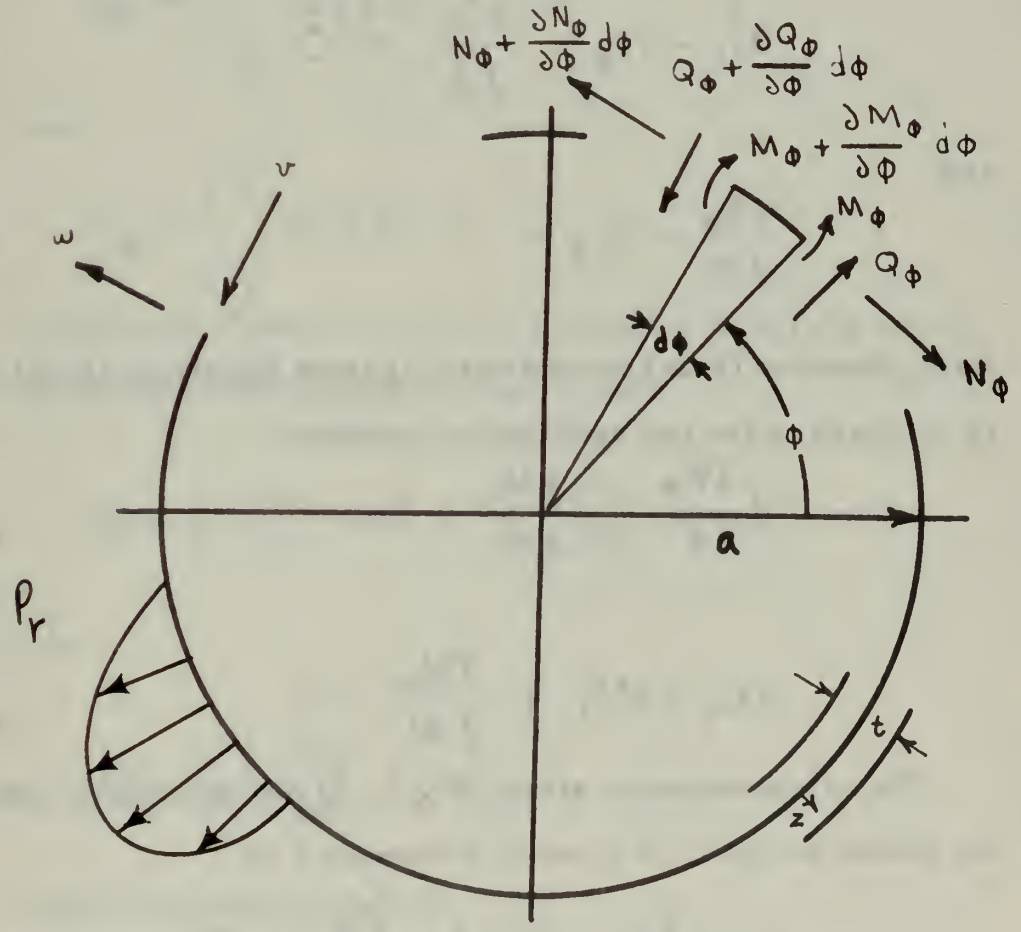

FIGURE 1

RING CONFIGURATION

the shear force Q_ϕ, the bending moment M_ϕ, and the applied radial loading P_r are shown in the positive direction. The displacements, also shown in the positive direction in Figure 1, are w in the radial direction and v in the tangential direction.

Assuming that the ring retains its circular shape after deformation, the equations of equilibrium can be written as

$$aQ_\phi - \frac{dM_\phi}{d\phi} = 0 \tag{2-1a}$$

$$aP_r - N_\phi - \frac{dQ_\phi}{d\phi} = 0 \tag{2-1b}$$

and

$$\frac{dN_\phi}{d\phi} - Q_\phi = 0 \tag{2-1c}$$

Using Equation (2-1a) to eliminate Q_ϕ from Equations (2-1b) and (2-1c) leads to the two equilibrium equations

$$a\frac{dN_\phi}{d\phi} - \frac{dM_\phi}{d\phi} = 0 \tag{2-2a}$$

$$aN_\phi - a^2P_r + \frac{d^2M_\phi}{d\phi^2} = 0 \tag{2-2b}$$

The circumferential strain, ε_ϕ, at any distance z from the middle surface, is given in Reference 1 as

$$\varepsilon_\phi = \frac{dv}{ad\phi} - \frac{z}{a}\frac{1}{(a+z)}\frac{d^2w}{d\phi^2} + \frac{w}{a+z} \tag{2-3}$$

This relationship is based upon the assumption that points on a normal to the middle surface prior to deformation remain on the

normal after deformation and that the thickness of the ring remains constant. Substituting Equation (2-3) into the plane stress form of the elastic constitutive law leads to

$$\sigma_\phi = E\left[\frac{dv}{a\,d\phi} - \frac{z}{a}\,\frac{1}{(a+z)}\,\frac{d^2w}{d\phi^2} + \frac{w}{a+z}\right] \tag{2-4}$$

where σ_ϕ is the circumferential stress at the location (ϕ, z) and E is the modulus of elasticity.

The normal force and bending moment are given by

$$N_\phi = \int_{-\frac{t}{2}}^{\frac{t}{2}} \sigma_\phi\, dz \tag{2-5a}$$

and

$$M_\phi = \int_{-\frac{t}{2}}^{\frac{t}{2}} \sigma_\phi\, z\, dz \tag{2-5b}$$

Substituting Equation (2-4) into Equations (2-5a) and (2-5b), integrating and applying the limits yield

$$N_\phi = \frac{D}{a}\left[\frac{dv}{d\phi} + w\right] + \frac{K}{a^3}\left[\frac{d^2w}{d\phi^2} + w\right] \tag{2-6a}$$

and

$$M_\phi = \frac{K}{a^2}\left[\frac{d^2w}{d\phi^2} + w\right] \tag{2-6b}$$

where $D = Et$ and $K = Et^3/12$. *

---

*In order to use this form of D and K the natural logarithmic terms that result from the integration of Equations (2-5a) and (2-5b) must be expanded in a series in terms of t/2a where terms to the fifth power and above are dropped.

The problem has now been reduced to one with four unknowns, v, w, N_ϕ, and M_ϕ, and four equations; two of the equations are obtained from the conditions of equilibrium

$$a\frac{dN_\phi}{d\phi} - \frac{dM_\phi}{d\phi} = 0 \tag{2-2a}$$

$$aN_\phi - a^2 P_r + \frac{d^2 M_\phi}{d\phi^2} = 0 \tag{2-2b}$$

and two are obtained from the application of the elastic constitutive law and the strain-displacement relationship

$$N_\phi = \frac{D}{a^2}\left[\frac{dv}{d\phi} + w\right] + \frac{K}{a^3}\left[\frac{d^2 w}{d\phi^2} + w\right] \tag{2-6a}$$

$$M_\phi = \frac{K}{a^2}\left[\frac{d^2 w}{d\phi^2} + w\right] \tag{2-6b}$$

Taking the appropriate derivatives with respect to ϕ of Equations (2-6a) and (2-6b) and substituting the results into Equations (2-2a) and (2-2b) yield

$$\frac{d}{d\phi}\left[\frac{dv}{d\phi} + w\right] = 0 \tag{2-7a}$$

and

$$\frac{dv}{d\phi} + w + k\left[\frac{d^4 w}{d\phi^4} + 2\frac{d^2 w}{d\phi^2} + w\right] - \frac{a^2 P_r}{D} = 0 \tag{2-7b}$$

where $k = t^2/12a^2$. Equations (2-7a) and (2-7b) are the governing differential equations for a thin ring under the assumptions that have been made.

CHAPTER III

DEVELOPMENT OF THE FOURIER SERIES SOLUTION TO THE GOVERNING EQUATIONS

The starting point in the development of the Fourier series solution to Equations (2-7a) and (2-7b) is to assume that the applied load, P_r, is a general function of ϕ, symmetrically distributed about two perpendicular planes, one through $\phi = 0$ and $0 = \pi$, and one through $0 = \pm\pi/2$. Thus, the load can be represented by the Fourier cosine series *

$$P_r = \sum_{m=0,2,4}^{\infty} P_m \cos m\phi \tag{3-1}$$

where the coefficients P_m are given by

$$P_o = \frac{1}{\pi}\int_o^{\pi} P_r \, d\phi \tag{3-2a}$$

and

$$P_m = \frac{2}{\pi}\int_o^{\pi} P_r \cos m\phi \, d\phi \tag{3-2b}$$

The radial displacement, w, which is an even function of ϕ for the ring under the load distribution considered, is also written in a Fourier cosine series as

$$w = \sum_{m=0,2,4}^{\infty} w_m \cos m\phi \tag{3-3}$$

---

* The symmetry conditions on P_r lead to the elimination of all odd values of m, i.e., $P_m = 0$ for all odd values of m.

The tangential displacement v is an odd function of ϕ and is given by

$$v = \sum_{m=2,4}^{\infty} v_m \sin m\phi \tag{3-4}$$

The governing differential equations are used to obtain w_m and v_m as a function of P_m. For the axisymmetric mode, where m = 0, the substitution of Equations (3-1) and (3-3) into Equation (2-7b) yields

$$w_o = \frac{a^2 P_o}{D(1+k)} \tag{3-5}$$

For the general case of $m > 0$, substitution of Equations (3-3) and (3-4) into Equation (2-7a) results in

$$m^2 v_m + m w_m = 0 \tag{3-6}$$

Substituting Equations (3-1), (3-3), and (3-6) into Equation (2-7b) gives

$$w_m = \frac{a^2 P_m}{k D (m^2-1)^2}$$

Therefore, according to Equation (3-6)

$$v_m = - \frac{a^2 P_m}{k D m (m^2-1)^2}$$

Substituting these expressions for w_m and v_m into Equations (3-3) and (3-4) leads to.

$$w = \frac{a^2 P_o}{D(1+k)} + \frac{a^2}{kD} \sum_{m=2,4}^{\infty} \frac{P_m \cos m\phi}{(m^2-1)^2} \tag{3-7a}$$

$$v = \frac{a^2}{k D} \sum_{m = 2,4}^{\infty} \frac{P_m}{m(m^2-1)^2} \qquad (3\text{-}7b)$$

All other quantities of interest are determined by using these expressions for w and v in the appropriate equations. For example, according to Equations (2-6a) and (2-6b), the normal force is given by

$$N_\phi = a P_o - a \sum_{m = 2,4}^{\infty} \frac{P_m \cos m\phi}{m^2 - 1} \qquad (3\text{-}8)$$

And the bending moment is

$$M_\phi = \frac{a^2 k P_o}{1+k} - a^2 \sum_{m = 2,4}^{\infty} \frac{P_m \cos m\phi}{m^2 - 1} \qquad (3\text{-}9)$$

To permit a direct comparison between the Fourier series and finite element analyses of the ring, w, N_ϕ, and M_ϕ, are selected for evaluation by both methods at the points $\phi = 0$, 30, 60, and 90 degrees. In Chapter IV, P_m, and the specific equations for w, N_ϕ, and M_ϕ are developed and evaluated at these values of ϕ for three different load conditions.

CHAPTER IV

APPLICATION AND RESULTS OF THE FOURIER SERIES SOLUTION

The three loads selected for use in this study are shown in Figure 2. All three loads are radial loads, directed inward, and are symmetrically distributed about two planes, one through $\phi = 0$ and $\phi = \pi$ and one through $\phi = \pm \pi/2$. Case 1 is a "line" or "knife edge" load of P pounds distributed over the width of the ring at $\phi = 0$ and $\phi = \pi$.

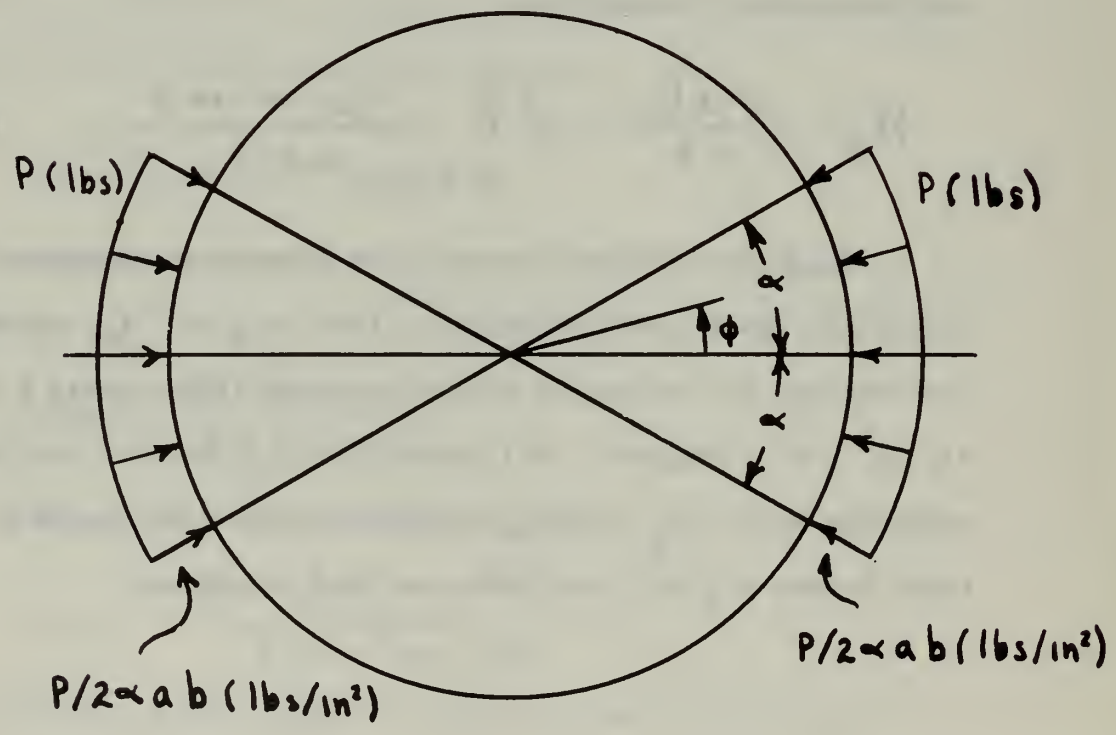

Case 1 α = 0 degrees

Case 2 α = 30 degrees

Case 3 α = 60 degrees

FIGURE 2

LOADS CONSIDERED

Case 2 and Case 3 loads are uniform pressure loads, each with a total value of P pounds covering the areas shown in Figure 2. The uniform loads are initially represented as P pounds distributed over the angle 2α so that the surface load P_r is given by

$$P_r = - \frac{P}{2\alpha ab} \tag{4-1}$$

Thus, substituting Equation (4-1) into Equation (3-1) gives

$$\frac{P}{2\alpha ab} = -\sum_{m=0,2,4}^{\infty} P_m \cos m\phi$$

Accordingly Equation (3-2a) becomes

$$P_o = - \frac{P}{2\alpha ab}\left[\int_0^{\alpha} d\phi + \int_{\pi-\alpha}^{\pi} d\phi \right]$$

so that

$$P_o = - \frac{P}{\pi ab} \tag{4-2}$$

Similiarly, substituting Equation (4-1) into Equation (3-2b), integrating and applying the limits yield

$$P_m = - \frac{P}{\pi ab m\alpha}\left[\sin m\alpha - \sin m(\pi-\alpha)\right]$$

Therefore

$$P_m = - \frac{2P \sin m\alpha}{\pi ab\, m\alpha} \tag{4-3}$$

for m even. For odd values of m

$$P_m = 0$$

as originally noted in Equation (3-1).

Applying Equation (4-2) and (4-3) to Equations (3-7a), (3-8) and (3-9) leads to the Fourier series solution for w, N_ϕ and M_ϕ

$$w = -\frac{aP}{\pi bD(1+k)} - \frac{2aP}{\pi bkD}\sum_{m=2,4}^{\infty}\frac{\sin m\alpha \cos m\phi}{\alpha m(m^2-1)^2} \qquad (4\text{-}4a)$$

$$N_\phi = -\frac{P}{\pi b} + \frac{2P}{\pi b}\sum_{m=2,4}^{\infty}\frac{\sin m\alpha \cos m\phi}{\alpha m(m^2-1)} \qquad (4\text{-}4b)$$

and

$$M_\phi = -\frac{akP}{\pi b(1+k)} + \frac{2aP}{\pi b}\sum_{m=2,4}^{\infty}\frac{\sin m\alpha \cos m\phi}{\alpha m(m^2-1)} \qquad (4\text{-}4c)$$

The non-dimensional forms of these three equations, denoted by $\bar{w}$, $\bar{N}_\phi$ and $\bar{M}_\phi$, and obtained by using $k = t^2/12a^2$, $D = Et$, and $I = bt^3/12$, are

$$\bar{w} = \frac{wEI}{a^3P} = -\frac{I}{\pi a^2 A(1+k)} - \frac{2}{\pi}\sum_{m=2,4}^{\infty}\frac{\sin m\alpha \cos m\phi}{\alpha m(m^2-1)^2} \qquad (4\text{-}5a)$$

$$\bar{N}_\phi = \frac{bN_\phi}{P} = -\frac{1}{\pi} + \sum_{m=2,4}^{\infty}\frac{\sin m\alpha \cos m\phi}{\alpha m(m^2-1)} \qquad (4\text{-}5b)$$

and

$$\bar{M}_\phi = \frac{bM_\phi}{aP} = -\frac{I}{\pi a^2 A(1+k)} + \frac{2}{\pi}\sum_{m=2,4}^{\infty}\frac{\sin m\alpha \cos m\phi}{\alpha m(m^2-1)} \qquad (4\text{-}5c)$$

These expressions are applicable only to Case 2 and 3 loads. For Case 1 load, $\alpha \rightarrow 0$. Thus, taking the limit of Equations (4-5a), (4-5b) and (4-5c) as $\alpha \rightarrow 0$ leads to the solution for Case 1 load

$$\bar{w} = -\frac{I}{\pi a^2 A(1+k)} - \frac{2}{\pi}\sum_{m=2,4}^{\infty} \frac{\cos m\phi}{(m^2-1)^2} \qquad (4\text{-}6a)$$

$$\bar{N}_\phi = -\frac{1}{\pi} - \frac{2}{\pi}\sum_{m=2,4}^{\infty} \frac{\cos m\phi}{m^2-1} \qquad (4\text{-}6b)$$

and

$$\bar{M}_\phi = -\frac{I}{\pi a^2 A(1+k)} - \frac{2}{\pi}\sum_{m=2,4}^{\infty} \frac{\cos m\phi}{m^2-1} \qquad (4\text{-}6c)$$

The term $-I/\pi a^2 A(1+k)$ that appears in w and M_ϕ will now be examined for its contribution and significance. The expressions

$$dU_a = \frac{N^2 a(d\phi)}{2AE} \quad \text{and} \quad dU_b = \frac{M^2 a(d\phi)}{2EI}$$

give the axial strain energy and the bending strain energy respectively of an element $b\,ta(d\phi)$ of the ring. They show that the axial strain energy is proportional to 1/A and the bending strain energy is proportional to 1/I. Using $U_a \approx 1/A$ and $U_b \approx 1/I$ leads to $U_a/U_b \approx I/A$. In Reference 2, the axial strain energy for such a curved element is shown to be very small compared to the

bending strain energy of the element provided that t/a is small.* Thus, the term $-I/\pi a^2 A(1+k)$ in $\bar{w}$ and $\bar{M}_\phi$ is related to the extension of the middle surface of the ring and should be small. If the middle surface is considered inextensional, the axial strain energy of an element of the ring is zero, and the term $-I/\pi a^2 A(1+k)$, which is proportional to U_a/U_b, does not appear in the expressions for $\bar{w}$ and $\bar{M}_\phi$. In order to determine the magnitude of the contribution of the axial strain energy to the solution, a t/a ratio must be selected. As an example, a ratio of t/a = 1/10 is chosen and $\bar{w}$ and $\bar{M}_\phi$ are calculated with and without the term containing I/A at ϕ = 0, 30, 60 and 90 degrees for all three load conditions. The results of these calculations are found in Table I, where the values referred to as "EXT" include the $-I/\pi a^2 A(1+k)$ term and the "NON-EXT" values do not. As is evident from Table I the differences between the "EXT" and "NON-EXT" values are very small, or nonexistent for the accuracy retained, when t/a = 10.

An important consideration in the application of the Fourier series method is the number of terms of the series required to give a desired accuracy in the solution, i.e., how fast does

---

*This statement assumes there are no distributed loads on the element, i.e., only concentrated loads are considered. This thesis considers distributed loads, and thus the statement is not completely applicable.

TABLE I

FOURIER SERIES EXTENSIONAL AND NON-EXTENSIONAL RESULTS

		CASE 1 LOAD		CASE 2 LOAD		CASE 3 LOAD	
ϕ		Ext.	Non-ext.	Ext.	Non-ext.	Ext.	Non-ext.
	$\bar{w}$	-0.0747	-0.0744	-0.0599	-0.0596	-0.0289	-0.0287
0°	$\bar{N}_\phi$	0.0	0.0	-0.128	-0.128	-0.239	-0.239
	$\bar{M}_\phi$	0.318	0.318	0.190	0.190	0.079	0.080
	$\bar{w}$	-0.0337	-0.0334	-0.0289	-0.0287	-0.0152	-0.0149
30°	$\bar{N}_\phi$	-0.250	-0.250	-0.239	-0.239	-0.271	-0.271
	$\bar{M}_\phi$	0.068	0.068	0.079	0.080	0.047	0.048
	$\bar{w}$	0.0361	0.0364	0.0295	0.0298	0.0141	0.0143
60°	$\bar{N}_\phi$	-0.433	-0.433	-0.413	-0.413	-0.358	-0.358
	$\bar{M}_\phi$	-0.115	-0.115	-0.095	-0.095	-0.040	-0.040
	$\bar{w}$	0.0680	0.0683	0.0571	0.0574	0.0295	0.0298
90°	$\bar{N}_\phi$	-0.500	-0.500	-0.477	-0.477	-0.413	-0.413
	$\bar{M}_\phi$	-0.182	-0.182	-0.159	-0.159	-0.095	-0.095

the series converge? This information for the inextensional form of the solution is shown in Tables II, III and IV for the first 4 terms of $\bar{w}$, $\bar{N}_\phi$ and $\bar{M}_\phi$ at $\phi = 0,\ 30,\ 60$ and 90 degrees for all three load conditions. The number of terms required for convergence of a series to four decimal place accuracy for the displacement and three decimal place accuracy for the forces and bending moments is shown in the last column with the converged value of the series.

TABLE II

FOURIER SERIES NON-EXTENSIONAL CONVERGENCE
FOR CASE 2 LOAD

Term		1	2	3	4	Converged
ϕ	m	2	4	6	8	Value
0°	$\sum \bar{w}_m$	-0.0707	-0.0736	-0.0741	-0.0742	-0.0744 at m = 14
	$\sum \bar{N}_m$	-0.106	-0.064	-0.045	-0.035	0.000 at m = 534
	$\sum \bar{M}_m$	0.212	0.255	0.273	0.283	0.318 at m = 394
30°	$\sum \bar{w}_m$	-0.0354	-0.0340	-0.0334		-0.0334 at m = 6
	$\sum \bar{N}_m$	-0.212	-0.233	-0.252	-0.257	-0.250 at m = 34
	$\sum \bar{M}_m$	0.106	0.085	0.067	0.062	0.068 at m = 52
60°	$\sum \bar{w}_m$	0.0354	0.0368	0.0363	0.0363	0.0364 at m = 14
	$\sum \bar{N}_m$	-0.424	-0.446	-0.427	-0.432	-0.433 at m = 24
	$\sum \bar{M}_m$	-0.106	-0.127	-0.109	-0.114	-0.115 at m = 38
90°	$\sum \bar{w}_m$	0.0707	0.0679	0.0684	0.0683	0.0683 at m = 8
	$\sum \bar{N}_m$	-0.531	-0.488	-0.506	-0.496	-0.500 at m = 26
	$\sum \bar{M}_m$	-0.212	-0.170	-0.188	-0.178	-0.182 at m = 38

TABLE III

FOURIER SERIES NON-EXTENSIONAL CONVERGENCE
FOR CASE 2 LOAD

Term		1	2	3	4	Converged
ϕ	m	2	4	6	8	Value
0^o	$\sum\bar{w}_m$	-0.058	-0.0547	-0.0597	-0.0596	-0.0596 at m = 8
	$\sum\bar{N}_m$	-0.143	-0.125	-0.125	-0.127	-0.128 at m = 10
	$\sum\bar{M}_m$	0.175	0.193	0.193	0.191	0.190 at m = 20
30^o	$\sum\bar{w}_m$	-0.0292	-0.0287			-0.0287 at m = 4
	$\sum\bar{N}_m$	-0.231	-0.239	-0.239	-0.238	-0.239 at m = 10
	$\sum\bar{M}_m$	0.088	0.079	0.079	0.080	0.080 at m = 14
60^o	$\sum\bar{w}_m$	0.0292	0.0298			0.0298 at m = 4
	$\sum\bar{N}_m$	-0.406	-0.415	-0.415	-0.414	-0.413 at m = 44
	$\sum\bar{M}_m$	-0.088	-0.097	-0.097	-0.095	-0.095 at m = 8
90^o	$\sum\bar{w}_m$	0.0585	0.0573	0.0573	0.0574	0.0574 at m = 8
	$\sum\bar{N}_m$	-0.494	-0.476	-0.476	-0.478	-0.477 at m = 10
	$\sum\bar{M}_m$	-0.175	-0.158	-0.158	-0.160	-0.159 at m = 10

TABLE IV

FOURIER SERIES NON-EXTENSIONAL CONVERGENCE
FOR CASE 3 LOAD

Term		1	2	3	4	Converged Value
0	m	2	4	6	8	
0°	$\sum \bar{w}_m$	-0.0292	-0.0287			-0.0287 at m = 4
	$\sum \bar{N}_m$	-0.231	-0.239	-0.239	-0.238	-0.239 at m = 10
	$\sum \bar{M}_m$	0.088	0.079	0.079	0.080	0.080 at m = 14
30°	$\sum \bar{w}_m$	-0.0146	-0.0149			-0.0149 at m = 4
	$\sum \bar{N}_m$	-0.274	-0.270	-0.270	-0.271	-0.271 at m = 8
	$\sum \bar{M}_m$	0.044	0.048	0.048	0.048	0.048 at m = 14
60°	$\sum \bar{w}_m$	0.0146	0.0143			0.0143 at m = 4
	$\sum \bar{N}_m$	-0.362	-0.358			-0.358 at m = 4
	$\sum \bar{M}_m$	-0.044	-0.039	-0.039	-0.040	-0.040 at m = 8
90°	$\sum \bar{w}_m$	0.0292	0.0298			0.0298 at m = 4
	$\sum \bar{N}_m$	-0.406	-0.415	-0.415	-0.414	-0.413 at m = 44
	$\sum \bar{M}_m$	-0.088	-0.097	-0.097	-0.095	-0.095 at m = 8

CHAPTER V

DEVELOPMENT OF THE FINITE ELEMENT SOLUTION

The finite element method is based upon the concept of replacing the actual continuous structure with a number of structural elements of finite size, leading to an assembled structure. The requirements of equilibrium and continuity at the element joints or nodes lead to a set of simultaneous algebraic equations. There are two general methods for formulating these equations, the displacement method and the force method. The displacement method, also known as the stiffness or direct stiffness method, is the one used in this thesis to solve the ring problem. This method is discussed in detail in Reference 3. A brief explanation of the method is given here for continuity.

In the displacement method the displacements and rotations at the nodes of the elements comprising the structure are taken as the unknown quantities. The matrix equation which relates the external forces to the displacements of an assembled structure is

$$\{X\} = [K]\{u\} + \{X^o\} \tag{5-1}$$

Matrix $\{X\}$ is the column matrix of nodal forces, i.e., forces that act upon the nodes of the element. In a general three dimensional structure these may include bending and twisting moments as well as rectilinear forces. The matrix $[K]$ is a square symmetric matrix for the entire structure. This matrix is known as the stiffness matrix and is assembled from the individual stiffness matrices of the elements forming the structure. The

entries in the element stiffness matrices are called stiffness influence coefficients. They are determined by displacing a node of the element by one unit in the direction of one of the degrees of freedom permitted for that node and calculating the nodal forces required to maintain that unit displacement and to prevent movement in any other degree of freedom for the nodes on the element. The amount of force required at a node to maintain this displacement state is one stiffness influence coefficient. The complete set of stiffness influence coefficients is determined by repeating this procedure for each degree of freedom at every node. The column matrix $\{u\}$ is the matrix of displacements and rotations which may take place at a node. The column matrix $\{X^o\}$ is a matrix of initial forces. They are determined by clamping all of the nodes of the assembled structure and calculating the external force required at each node to maintain this zero displacement state under the applied load condition. Thus, loads distributed between nodes and concentrated loads not located at nodes can be treated.

There are various techniques available for the manipulation and solution of Equation (5-1). The one used in this study is to transpose $\{X^o\}$ to the left-hand side of Equation (5-1). This leads to a single column matrix of forces $\left\{\{X\} - \{X^o\}\right\}$. Next, the matrix equation is reduced in order by a consideration of the boundary conditions on the structure. If the boundary conditions specify zero displacement at some nodes, then those nodal displacements are no longer unknowns and are removed from $\{u\}$ along with the row of the equation and the column of $[K]$ that

correspond to that zero displacement. The remaining matrix equation, which is referred to as the reduced matrix equation and is subscripted with ρ, is

$$\left\{X_\rho\right\} - \left\{X^o_\rho\right\} = \left[K_\rho\right]\left\{u_\rho\right\} \tag{5-2}$$

The unknowns in Equation (5-2) are contained in the matrix of displacements $\left\{u_\rho\right\}$. Equation (5-2) is a set of simultaneous linear algebraic equations that is solved on a digital computer using the FORTRAN IV subroutine "DSIMQ," a description of which appears in Appendix C. The outputs of "DSIMQ" are the nodal displacements $\left\{u_\rho\right\}$.

In order to determine the nodal forces $\left\{X\right\}$, the stiffness matrix equation is solved for each element. These equations, subscripted η, are

$$\left\{X_\eta\right\} = \left[K_\eta\right]\left\{u_\eta\right\} + \left\{X^o_\eta\right\} \tag{5-3}$$

The unknowns in this equation are in $\left\{X_\eta\right\}$ since the displacements $\left\{u_\eta\right\}$ are obtained from the appropriate locations in $\left\{u_\rho\right\}$ and $\left\{u\right\}$. The matrix $\left\{X_\eta\right\}$ is obtained by adding the matrix $\left\{X^o_\eta\right\}$, which is determined by selecting values from appropriate locations in $\left\{X^o\right\}$, to the matrix $\left[K_\eta\right]\left\{u_\eta\right\}$. With $\left\{u_\eta\right\}$ and $\left\{X_\eta\right\}$ known, all of the nodal displacements and forces have been determined, and the problem is solved since the forces and displacements at any interior location of an element can be determined from the applied load and nodal forces and displacements.

Applying the finite element method to the ring problem under consideration requires the selection of the element geometry. Either straight or curved elements can be used. Curved elements are selected since they more naturally match the shape of the ring and result in displacements and forces that are readily interpreted without requiring a change in coordinates. The curved element used is drawn in Figure 3 with the nodal forces N_1, Q_1, N_2, Q_2, bending moments M_1, M_2, displacements w_1, v_1, w_2, v_2 and rotations θ_1, θ_2 shown in the positive sense. The element covers the angle β. A stiffness matrix for this element has been derived in Reference 3* based on the assumption that the thickness of the element, t, is small compared to the radius of

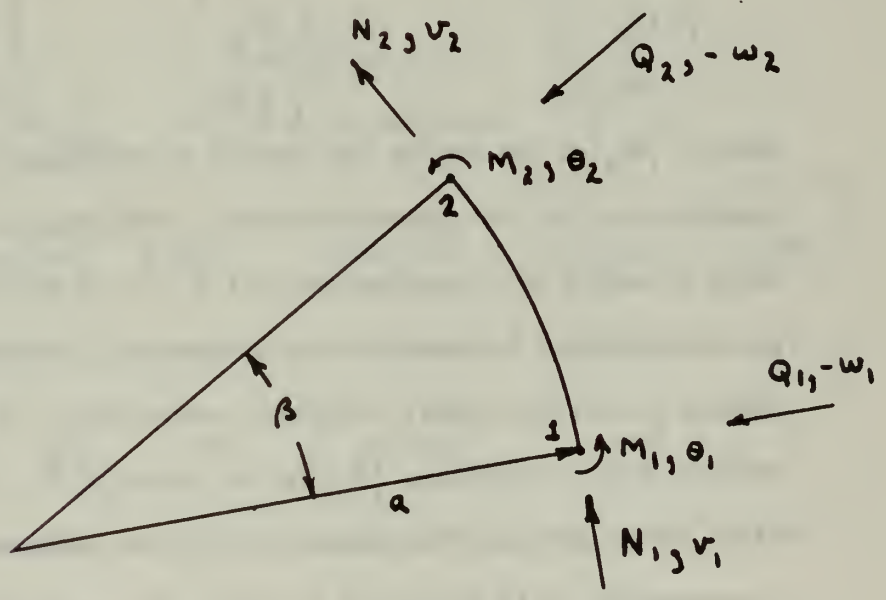

FIGURE 3

FINITE ELEMENT CONFIGURATION

*A more detailed derivation and a comprehensive study of the curved element appear in Reference 4.

curvature, a, so that only the strain energy of bending need be considered during the derivation. This assumption neglects the shear distortion energy, the energy resulting from any coupling between bending moment and normal force, the energy of axial deformation, and the displacements that correspond to these three forms of strain energy. The stiffness matrix equation from Reference 3 for the curved element can be given in a form corresponding to Equation (5-2) as

$$\begin{Bmatrix} N_1 \\ Q_1 \\ M_1/a \\ N_2 \\ Q_2 \\ M_2/a \end{Bmatrix} = \frac{EI}{a^3} \left[K_\eta\right] \begin{Bmatrix} v_1 \\ -w_1 \\ a\theta_1 \\ v_2 \\ -w_2 \\ a\theta_2 \end{Bmatrix} + \begin{Bmatrix} N_1^o \\ Q_1^o \\ M_1^o/a \\ N_2^o \\ Q_2^o \\ M_2^o/a \end{Bmatrix} \quad (5\text{-}4)$$

where $\left[K_\eta\right]$ is the six by six matrix of stiffness influence coefficients for the curved element. The matrix $\left[K_\eta\right]$, each term of which is a function only of β, will not be written out in functional form because it is quite lengthy. For this thesis a double precision digital computer subroutine, "RELM," was written which computes $\left[K_\eta\right]$ for an input of β. A copy of "RELM" is included in Appendix C. The stiffness matrix $\left[K_\eta\right]$ computed by "RELM" for $\beta = 7.5$, 15, and 30 degrees is presented in Tables V, VI and VII respectively.

With $\left[K_\eta\right]$ determined, $\left[K\right]$ can be assembled. Equation (5-1) is completed for the ring by using the loading conditions to obtain $\left\{X^o\right\}$ and the appropriate portions of $\left\{X\right\}$. Because of the

TABLE V

$[K_\eta]$ for $\beta = 7.5$ degrees

18,665,685	1,223,063	26,675	-18,665,640	1,223,762	-26,721
1,223,063	85,518	2,099	-1,223,762	74,855	-1,400
26,675	2,099	69	26,721	1,400	-23
-18,665,640	-1,223,762	-26,721	18,665,685	-1,223,063	26,675
1,223,762	74,855	1,400	-1,223,063	85,518	-2,099
-26,721	-1,400	-23	26,675	-2,099	69

TABLE VI

$[K_\eta]$ for $\beta = 15$ degrees

576,897	75,862	3,306	-576,874	76,035	-3,329
75,862	10,658	524	-76,035	9,339	-350
3,306	524	34	-3,329	340	-11
-576,874	-76,035	-3,329	576,897	-75,862	3,306
76,035	9,339	350	-75,862	10,658	-524
-3,329	-350	-11	3,306	-524	34

TABLE VII

$[K_\eta]$ for $\beta = 30$ degrees

17,243	4,598	399	-17,232	4,640	-411
4,598	1,317	130	-4,640	1,158	-87
399	130	17	-411	87	-6
-17,323	-4,640	-411	17,243	-4,598	399
4,640	1,158	87	-4,598	1,317	-130
-411	-87	-6	399	-130	17

symmetrical nature of the applied loads only one quadrant of the ring needs to be considered. The quadrant from $\phi = 0$ to 90 degrees is selected so that a direct comparison with the Fourier series solution for $\bar{w}$, $\bar{N}_\phi$ and $\bar{M}_\phi$ can be made for $\phi = 0$, 30, 60 and 90 degrees.

CHAPTER VI

APPLICATION AND RESULTS OF THE FINITE ELEMENT SOLUTION

In order to apply the finite element solution to the ring quadrant ϕ = 0 to 90 degrees, Equation (5-1) is assembled for the entire quadrant using Equation (5-4) for each of the elements comprising the quadrant. $[K_\eta]$ matrices for β = 7.5, 15 and 30 degrees are used in this thesis so that the quadrant is divided into 12, 6 and 3 elements respectively for the solution of each of the three load conditions. This assembled equation is reduced and solved in the manner described in Chapter V. The process of assembling, reducing, and solving Equation (5-4) is best described by using an example. Case 2 load with β = 30 degrees is selected as the example.

Figure 4 shows the assembled quadrant and the node numbering sequence for the three elements in the quadrant. For three

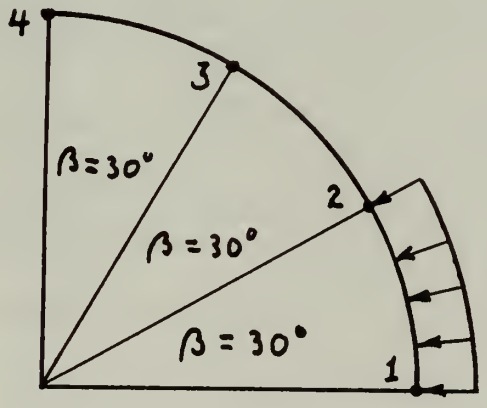

FIGURE 4

3 ELEMENT QUADRANT FOR CASE 2 LOAD

elements $[K]$ is a 12 x 12 square symmetric matrix which is assembled using three of the 6 x 6 $[K_n]$ matrices from Table VII.

When assembled for this example, Equation (5-1) appears as

$$\begin{Bmatrix} N_1 \\ Q_1 = 0 \\ M_1/a \\ N_2 = 0 \\ Q_2 = 0 \\ M_2/a = 0 \\ N_3 = 0 \\ Q_3 = 0 \\ M_3/a \\ N_4 \\ Q_4 = 0 \\ M_4/a \end{Bmatrix} = \frac{EI}{a^3} [K]_{12 \times 12} \begin{Bmatrix} v_1 = 0 \\ -w_1 \\ a\theta_1 = 0 \\ v_2 \\ -w_2 \\ a\theta_2 \\ v_3 \\ -w_3 \\ a\theta_3 \\ v_4 = 0 \\ -w_4 \\ a\theta_4 = 0 \end{Bmatrix} + \begin{Bmatrix} N_1^o \\ Q_1^o \\ M_1^o/a \\ N_2^o \\ Q_2^o \\ M_2^o/a \\ N_3^o \\ Q_3^o \\ M_3^o/a \\ N_4^o \\ Q_4^o \\ M_4^o/a \end{Bmatrix} \qquad (6\text{-}1)$$

where the zero entries in the $\{X\}$ and $\{u\}$ matrices are obtained from the symmetry characteristics of the load. The initial forces in $\{X^o\}$ are derived in Appendix B and presented in Table BI. They are transposed to the left-hand side of Equation (6-1) to give

$$\begin{Bmatrix} N_1 - .12709678 \\ 0 - .22182251 \\ M_2/a - .01944670 \\ 0 - .12707678 \\ 0 - .22182251 \\ 0 - .01944670 \\ 0 \\ 0 \\ 0 \\ N_4 \\ 0 \\ M_4/a \end{Bmatrix} = \frac{EI}{a^3} \left[K\right] 12 \times 12 \begin{Bmatrix} 0 \\ -w_1 \\ 0 \\ v_2 \\ -w_2 \\ a\theta_2 \\ v_3 \\ -w_3 \\ a\theta_3 \\ 0 \\ -w_4 \\ 0 \end{Bmatrix} \qquad (6\text{-}2)$$

The reduced matrix equation is created from Equation (6-2) by striking out the rows of the equation and columns of $\left[K\right]$ 12 x 12. The reduced equation with $\left[K\rho\right]$ an 8 x 8 matrix appears in Table VIII.

A computer program, "BETA 30," a copy of which appears in Appendix C, solves Equation (6-3) for $\left\{u\rho\right\}$ by using the subroutine "DSIMQ." For this example the output of "DSIMQ" is

$$\bar{w}_1 = \frac{w_1 EI}{a^3 P} = -0.0596$$

$$\bar{v}_2 = \frac{v_2 EI}{a^3 P} = 0.0255$$

$$\bar{w}_2 = \frac{w_2 EI}{a^3 P} = -0.0287$$

$$\bar{\theta}_2 = \frac{\theta_2 EI}{a^2 P} = -0.0802$$

TABLE VIII

REDUCED MATRIX EQUATION FOR CASE 2 LOAD, β = 30 DEGREES

$$\begin{Bmatrix} 0.22182251P \\ 0.12707678P \\ 0.22182251P \\ -0.01944670P \\ 0.0 \\ 0.0 \\ 0.0 \\ 0.0 \end{Bmatrix} = \frac{EI}{a^3} \begin{bmatrix} 1,317 & -4,640 & 1,158 & -87 & 0 & 0 & 0 & 0 \\ -4,640 & 34,487 & 0 & 798 & -17,232 & 4,640 & -411 & 0 \\ 1,158 & 0 & 2,633 & 0 & -4,640 & 1,158 & -87 & 0 \\ -87 & 798 & 0 & 34 & -411 & 87 & -6 & 0 \\ 0 & -17,232 & -4,640 & -411 & 34,487 & 0 & 798 & 4,640 \\ 0 & 4,640 & 1,158 & 87 & 0 & 2,633 & 0 & 1,158 \\ 0 & -411 & -87 & -6 & 798 & 0 & 34 & 87 \\ 0 & 0 & 0 & 0 & 4,640 & 1,158 & 87 & 1,317 \end{bmatrix} \begin{Bmatrix} -w_1 \\ v_2 \\ -w_2 \\ a\theta_2 \\ v_3 \\ -w_3 \\ a\theta_3 \\ -w_4 \end{Bmatrix}$$

TABLE IX

FINITE ELEMENT RESULTS FOR CASE 1 LOAD

ϕ		$\beta = 7.5^\circ$	$\beta = 15^\circ$	$\beta = 30^\circ$
0°	$\bar{w}$	-0.0744	-0.0744	-0.0744
	$\bar{N}_\phi$	0.000	0.000	0.000
	$\bar{M}_o$	0.318	0.318	0.318
30°	$\bar{w}$	-0.0334	-0.0334	-0.0334
	$\bar{N}_\phi$	-0.250	-0.250	-0.250
	$\bar{M}_\phi$	0.068	0.068	0.068
60°	$\bar{w}$	0.0364	0.0364	0.0364
	$\bar{N}_\phi$	-0.433	-0.433	-0.433
	$\bar{M}_\phi$	-0.115	-0.115	-0.115
90°	$\bar{w}$	0.0683	0.0683	-0.0683
	$\bar{N}_\phi$	-0.500	-0.500	-0.500
	$\bar{M}_\phi$	-0.182	-0.182	-0.182

TABLE X

FINITE ELEMENT RESULTS FOR CASE 2 LOAD

ϕ		$\beta = 7.5^{o}$	$\beta = 15^{o}$	$\beta = 30^{o}$
0^{o}	$\bar{w}$	-0.0596	-0.0596	-0.0596
	$\bar{N}_{\phi}$	-0.128	-0.128	-0.128
	$\bar{M}_{\phi}$	0.190	0.190	0.190
30^{o}	$\bar{w}$	-0.0287	-0.0287	-0.0287
	$\bar{N}_{\phi}$	-0.239	-0.239	-0.239
	$\bar{M}_{\phi}$	0.080	0.080	0.080
60^{o}	$\bar{w}$	0.0298	0.0298	0.298
	$\bar{N}_{\phi}$	-0.413	-0.413	-0.413
	$\bar{M}_{\phi}$	-0.095	-0.095	-0.095
90^{o}	$\bar{w}$	0.0574	0.573	-0.0573
	$\bar{N}_{\phi}$	-0.477	-0.477	-0.477
	$\bar{M}_{\phi}$	-0.159	-0.159	-0.159

TABLE XI

FINITE ELEMENT RESULTS FOR CASE 3 LOAD

ϕ		$\beta = 7.5^\circ$	$\beta = 15^\circ$	$\beta = 30^\circ$
0°	$\bar{w}$	-0.0287	-0.0287	-0.0287
	$\bar{N}_\phi$	-0.239	-0.239	-0.239
	$\bar{M}_\phi$	0.080	0.080	0.080
30°	$\bar{w}$	-0.0149	-0.0149	-0.0149
	$\bar{N}_\phi$	-0.271	-0.271	-0.271
	$\bar{M}_\phi$	0.048	0.048	0.048
60°	$\bar{w}$	0.0143	0.0143	0.0143
	$\bar{N}_\phi$	-0.358	-0.358	-0.358
	$\bar{M}_\phi$	-0.040	-0.040	-0.040
90°	$\bar{w}$	0.0298	0.0298	-0.0298
	$\bar{N}_\phi$	-0.413	-0.413	-0.413
	$\bar{M}_\phi$	-0.095	-0.095	-0.095

CHAPTER VII

COMPARISON AND DISCUSSION OF THE RESULTS

In order to provide a standard to which the results of the Fourier series and finite element methods can be compared, the ring problem is solved analytically for $\bar{N}_\phi$ and $\bar{M}_\phi$ in Appendix A for the three load conditions. The results of this analytical solution are non-dimensionalized and are entered in Tables XII, XIII and XIV with the results from the Fourier series and finite element methods. The Fourier series values in these three tables are the converged values of $\bar{w}$, $\bar{N}_\phi$ and $\bar{M}_\phi$, while the finite element values are the same quantities obtained by using $\beta = 7.5$ degrees. A comparison of the results entered in Tables XII, XIII and XIV shows essentially zero error. This is well within normal engineering tolerances for structural analysis and indicates that under proper conditions either of the two methods is capable of satisfactory accuracy.

Since accuracy alone does not provide a sufficient basis for choosing one method over the other, the convenience or ease of usage of each method must be examined. Ease of usage must be considered within the framework of the load applied, the accuracy desired, the equipment available, and the assumptions made. A comparison of the ease of usage of the two methods within the framework of the load applied reveals that the Fourier series method has distinct advantages over the finite element method when solving the ring problem for a load that is applied over the surface of the ring in such a manner that P_m is a function that is easily evaluated for changing m and ϕ. There are two reasons for this.

TABLE XII

RESULTS FOR CASE 1 LOAD

ϕ		Fourier Series	Finite Element	Analytical
0°	$\bar{w}$	-0.0744	-0.0744	-
	$\bar{N}_\phi$	0.000	0.000	0.000
	$\bar{M}_\phi$	0.318	0.318	0.318
30°	$\bar{w}$	-0.0334	-0.0334	-
	$\bar{N}_\phi$	-0.250	-0.250	-0.250
	$\bar{M}_\phi$	0.068	0.068	0.068
60°	$\bar{w}$	0.0364	0.0364	-
	$\bar{N}_\phi$	-0.433	-0.433	-0.433
	$\bar{M}_\phi$	-0.115	-0.115	-0.115
90°	$\bar{w}$	0.0683	0.0683	-
	$\bar{N}_\phi$	-0.500	-0.500	-0.500
	$\bar{M}_\phi$	-0.182	-0.182	-0.182

TABLE XIII

RESULTS FOR CASE 2 LOAD

ϕ		Fourier Series	Finite Element	Analytical
	$\bar{w}$	-0.0596	-0.0596	-
0^o	$\bar{N}_\phi$	-0.128	-0.128	-0.128
	$\bar{M}_\phi$	0.190	0.190	0.190
	$\bar{w}$	-0.0287	-0.0287	-
30^o	$\bar{N}_\phi$	-0.239	-0.239	-0.239
	$\bar{M}_\phi$	0.080	0.080	0.080
	$\bar{w}$	0.0298	0.0298	-
60^o	$\bar{N}_\phi$	-0.413	-0.413	-0.413
	$\bar{M}_\phi$	-0.095	-0.095	-0.095
	$\bar{w}$	0.0574	0.0574	-
90^o	$\bar{N}_\phi$	-0.477	-0.477	-0.477
	$\bar{M}_\phi$	-0.159	-0.159	-0.159

TABLE XIV

RESULTS FOR CASE 3 LOAD

ϕ		Fourier Series	Finite Element	Analytical
0^o	$\bar{w}$	-0.0287	-0.0287	-
	$\bar{N}_\phi$	-0.239	-0.239	-0.239
	$\bar{M}_\phi$	0.080	0.080	0.080
30^o	$\bar{w}$	-0.0149	-0.0149	-
	$\bar{N}_\phi$	-0.271	-0.271	-0.271
	$\bar{M}_\phi$	0.048	0.048	0.048
60^o	$\bar{w}$	0.0143	0.0143	-
	$\bar{N}_\phi$	-0.358	-0.358	-0.358
	$\bar{M}_\phi$	-0.040	-0.040	-0.040
90^o	$\bar{w}$	0.0298	0.0298	-
	$\bar{N}_\phi$	-0.413	-0.413	-0.413
	$\bar{M}_\phi$	-0.095	-0.095	-0.095

The first is that the series is easily evaluated when P_m is a simple function. The second is that for distributed loads the finite element method required initial fixed end conditions for those elements containing the loads. Unless these initial end conditions are available from a handbook or other source, they must be calculated using energy principles or some other method. As can be seen in Appendix B, calculation of these initial end conditions may be laborious and time consuming and may require a high degree of initial accuracy for the results to be useful. Even if the equations for calculating the initial end conditions are available in a handbook, they may be lengthy and may also require a high degree of initial accuracy.

A situation in which the finite element method is superior, in the framework of the load applied, is one where the load conditions lead to either $\{X^o\} = 0$ initial end conditions or fixed end conditions that are available and easily calculated. This is especially significant if several such loading conditions are to be considered. All that is required for a solution in such a situation, once a computer program has been written, is to change the program inputs to reflect the changes in $\{X\}$, $\{X^o\}$ and $\{u\}$ caused by the load change and to run the program for each loading condition. If the Fourier series method is used in this situation, each load change requires an integration to obtain P_m, and a different series must be calculated for each loading condition.

As pointed out earlier in this chapter, both methods are capable of giving excellent accuracy under certain conditions.

For the Fourier series method, accuracy is affected only by the number of terms included in the summation process. For displacements, Tables II, III and IV show that very few terms are required for a high degree of accuracy especially when a distributed load is applied. Using only 4 terms in any of the summations for $\bar{w}$, including that for the point load, gives a maximum error of 0.02 per cent. For $\bar{N}_\phi$ and $\bar{M}_\phi$ the situation is not quite as favorable, but at the worst, 4 terms give a maximum error of 3.5 per cent. If this degree of accuracy is satisfactory, the Fourier series method must be considered easier to use than the finite element method.

For the finite element method, all element sizes considered gave essentially the same results for all three load conditions. However, for load conditions other than the ones considered here, the analyst may be required to use elements with β less than 7.5 degrees. There appear to be two limiting factors on the minimum size of elements that can be used. The first limiting factor is computer capacity. As the elements are made smaller, more nodes are created, and hence larger matrices are required. When dealing with full scale structures, the limit of computer capacity can be reached prior to reaching the optimum element size for accuracy. The other limiting factor is related to computer capacity but arises from a characteristic of the curved element stiffness matrix rather than from the number of elements used. The characteristic referred to is the tendency for some of the numbers in the stiffness matrices, particularly on the main diagonal, to have a greater disparity in size as β is decreased. Tables V, VI and VII show this to a marked degree. For instance, the

ratio of the stiffness coefficient (6, 6) to coefficient (1, 1) in $[K_\eta]$ for $\beta = 30$ degrees is 17/17,243, whereas the ratio of the same two elements is 69/18,665,685 for $\beta = 7.5$ degrees. Since the computer retains only a certain number of significant figures while manipulating these matrices, a point will be reached where round-off error in computer operations will negate any gain in accuracy obtained by using smaller elements. This problem is alleviated to a degree by using double-precision techniques, as used in this thesis; but again since double-precision operations require more computer storage space, the computer capacity itself places a limit on this approach.

The equipment available to the analyst has a significant effect on the ease of usage of the two methods. Indeed, in the case of the finite element method, lack of a digital computer almost prohibits use of the method on the basis of effort required. Even if a digital computer is available, a desk calculator and a set of mathematical or trigonometric tables with up to ten significant figures is desirable if the nature of the load is such that fixed end conditions must be determined. On the other hand, while a desk calculator, and even a digital computer, may be used to advantage in the Fourier series method, neither are required. A slide-rule, a table of integrals, and normal trigonometric tables are sufficient equipment for application of the Fourier series method.

Finally, the ease of usage must be considered within the framework of the theory employed. The assumptions made when applying the two methods of solution to the ring can have an effect

on both the accuracy obtained and the ease of usage. The governing differential equations are derived, and the Fourier series solution developed through Equation (4-6a), (4-6b) and (4-6c) without making any assumptions regarding the extension of the middle surface of the ring. If the assumption is made during the derivation of these differential equations that the middle surface is inextensional, that is $\epsilon_\phi = 0$ when $z = 0$, then $\frac{dv}{d\phi} = -w$ and the $m = 0$, or extensional, terms do not appear in the expressions for w and M_ϕ.* As seen in Table I, no large error is introduced in $\bar{w}$ and $\bar{M}_\phi$ by this assumption. However, if this inextensional form of w is used in Equation (2-6a) to obtain N_ϕ, the resulting expression is missing the leading, or $m = 0$, term, and the values for N_ϕ calculated from this shortened expression are in unacceptable error. This problem may be circumvented by using the equilibrium equation, Equation (2-2a), to calculate N_ϕ.** The procedure used is to substitute the inextensional form of M_ϕ, obtained from Equation (2-6b), into Equation (2-2a) and integrate. The constant of integration is obtained from equilibrium considerations at one of the planes of symmetry. The resulting expression for N_ϕ is identical to Equation (4-4b) and thus gives accurate results. On the other hand, in the finite element method, an error will occur in the

---

* The governing equations for the modes $m \geq 2$ identically satisfy the inextensional assumption. Thus, these nodes are not affected by the assumption.

** This is analgous to determining Q_ϕ from the equilibrium equation, Equation (1-1a).

solution for w if the inextensional assumption is made and distributed loads are applied over almost all the ring surface. The reason for this is that a distributed load acting on the surface of a curved element has a greater tendency to compress or extend the middle surface than does a concentrated load. Errors are caused if the energy of this middle surface compression or extension is neglected, as it is in the derivation of the curved element stiffness matrix. Unlike the Fourier series method, there is no means of introducing this extensional behavior into the finite element method once the stiffness matrix is derived. The only recourse is to select a t/a ratio and re-derive the curved element stiffness matrix including the axial strain energy term in the calculations.

CHAPTER VIII

CONCLUSIONS AND RECOMMENDATIONS

The primary advantage of the Fourier series method for analyzing ring structures is that it gives reasonably accurate answers with a minimum amount of effort using a slide rule and normally available integral and trigonometric tables.

The primary advantage of the finite element method lies in its ability to accurately solve several different loading conditions with a minimum amount of effort. The finite element method has the disadvantage of requiring the calculation of fixed end conditions for certain types of loads.

A recommendation for further work is the derivation of a stiffness matrix for a curved element that includes the effects of axial strain energy. Also recommended is a matrix error analysis on both the extensional and inextensional forms of the curved element stiffness matrix for various values of the central angle.

REFERENCES

1. Flugge, Wilhelm, Stresses in Shells, Springer-Verlag, Berlin, 1960.
2. Timoshenko, S., Strength of Materials Part I, D. Van Nostrand Company, Inc., Princeton, New Jersey, Third Edition, 1955.
3. Martin, Harold C., Introduction to Matrix Methods of Structural Analysis, McGraw-Hill Book Company, New York, 1966.
4. Rasanen, George K.,"Analysis of Curved Bars", MS Thesis, University of Washington, 1962.
5. Timoshenko, S. and Woinowsky-Krieger, S., Theory of Plates and Shells, McGraw-Hill Book Company, New York, 1959.

APPENDIX A

ANALYTICAL SOLUTION

The ring problem is solved analytically for $\bar{N}_\phi$ and $\bar{M}_\phi$ for all three load conditions to obtain a standard to which the Fourier series and finite element results can be compared. The analytical solution is based on the symmetric character of the loads applied, the principle of superposition and Castigliano's Theorem. The use of superposition in the solution of thin shell problems is discussed in detail in Reference 5. Figure A 1 (I) shows the entire ring with an applied load of P pounds uniformly distributed over each of the two surface areas subtended by the angle 2α. Figures A 1 (II), (III) and (IV) show the portions of the ring that are superimposed to obtain a solution.

Considering the quadrant of the ring for $0 \leq \phi \leq \pi/2$, the boundary conditions plus equilibrium for Figure A 1 (II) require that

$$(N_\phi)_{II} = - P/2\alpha \qquad \text{(A-1a)}$$

and

$$(M_\phi)_{II} = - 0 \qquad \text{(A-1b)}$$

for $0 \leq \phi \leq \alpha$. Similarly

$$(N_\phi)_{III} = H_2 \cos \phi \qquad \text{(A-2a)}$$

and

$$(M_\phi)_{III} = M_2 + aH_2 (\cos \phi - \cos \alpha) \qquad \text{(A-2b)}$$

for Figure A 1 (III).

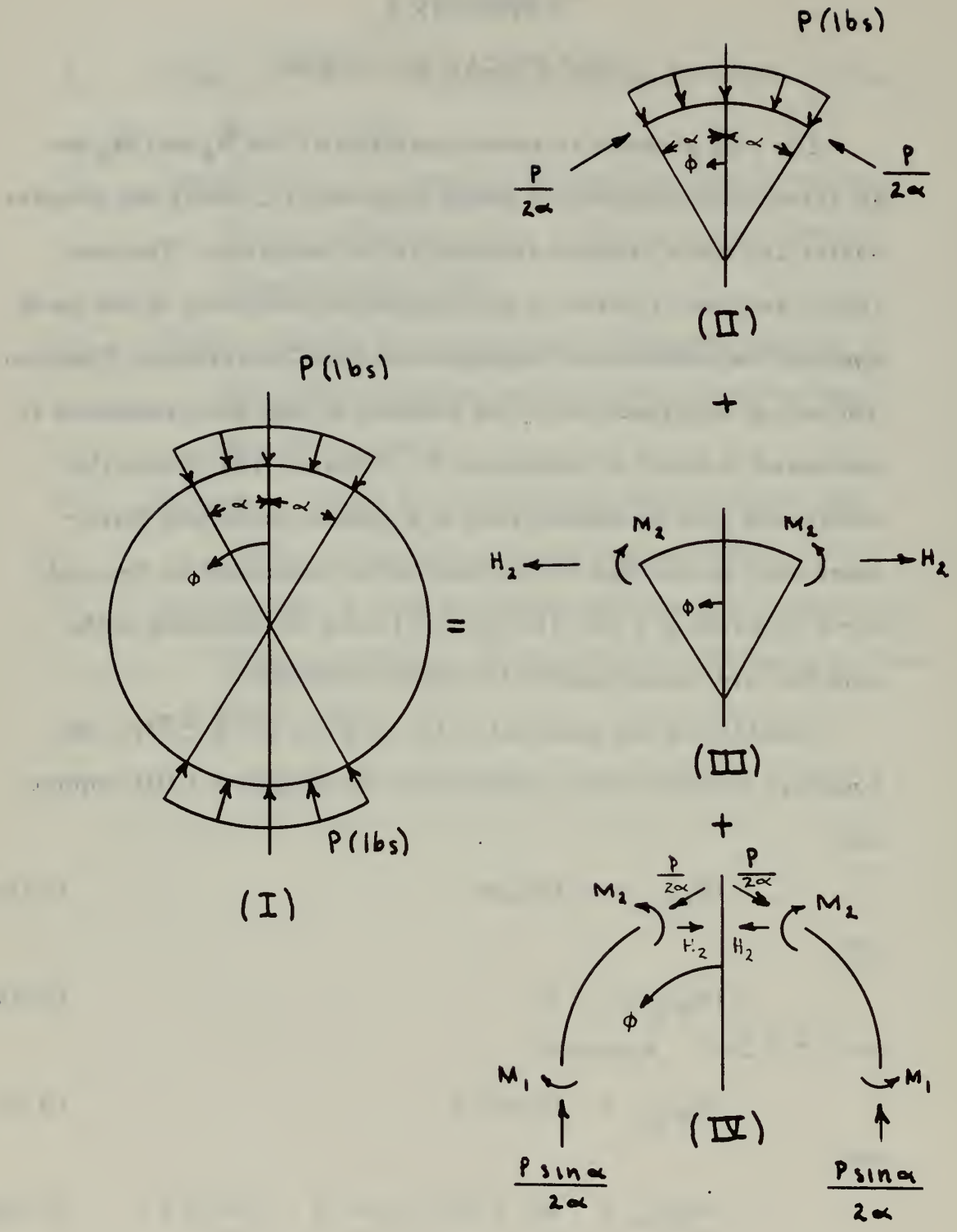

FIGURE A 1

RING SEGMENTS USED IN ANALYTICAL SOLUTION

In Figure A 1 (IV)

$$(N_\phi)_{IV} = -\frac{P \sin\alpha \sin\phi}{2\alpha} \qquad (A-3a)$$

and

$$(M_\phi)_{IV} = M_1 + \frac{a\,P \sin\alpha\,(1-\sin\phi)}{2\alpha}$$

are written for $\alpha \leq \phi \leq \pi/2$. Since equilibrium gives

$$M_1 = M_2 - aH_2 \cos\alpha - \frac{aP\,(1-\sin\alpha)}{2\alpha}$$

M_1 can be substituted in the expression for $(M_\phi)_{IV}$ to obtain

$$(M_\phi)_{IV} = M_2 - a\,H_2 \cos\alpha + \frac{aP\,(1-\sin\alpha \sin\phi)}{2\alpha} \qquad (A-3b)$$

When $\phi = \alpha$

$$M_\phi = M_2$$

so that Equation (A-3b) yields

$$H_2 = \frac{P\cos\alpha}{2\alpha}$$

This expression is substituted into Equations (A-2a) and (A-2b), and the resulting equations are superimposed on Equations (A-1a) and (A-1b) to obtain

$$N_\phi = \frac{P}{2\alpha}(\cos\alpha \cos\phi - 1) \qquad (A-4a)$$

and

$$M_\phi = M_2 + \frac{a\,P\cos\alpha}{2\alpha}(\cos\phi - \cos\alpha) \qquad (A-4b)$$

for $0 \leq \phi \leq \alpha$.

Substituting the same expression into Equation (A-3b) yields

$$M_\phi = M_2 + \frac{a\,P \sin}{2}(\sin\alpha - \sin\phi) \qquad (A-5)$$

where $\alpha \leq \phi \leq \pi/2$.

Castigliano's Theorem is applied in the form of

$\partial U_t / \partial M_2 = 0$ to obtain the internal moment M_2. The total strain energy, U_t, of the three segments is written as

$$U_t = U_{IIa} + U_{IIb} + U_{IIIa} + U_{IIIb} + U_{IVa} + U_{IVb}$$

where subscripts a and b stand for axial and bending strain energy respectively. The terms U_{IIa}, U_{IIb}, U_{IIIa}, and U_{IVa} need not be considered when applying Castigliano's Theorem to obtain M_2 since these terms are either zero or are not functions of M_2. Therefore $\partial U_t / \partial M_2 = 0$ becomes

$$\frac{\partial}{\partial M_2}\left[\int_0^{\alpha} \frac{M_\phi^2}{2EI}\, a\,d\phi + \int_{\alpha}^{\pi/2} \frac{M_\phi^2}{2EI}\, a\,d\phi\right] = 0 \qquad \text{(A-6)}$$

where the expressions for M_ϕ are obtained from Equations (A-4b) for the first integral and (A-5) for the second integral. Performing the partial differentiation and integration with the appropriate limits as indicated in Equation (A-6) gives

$$M_2 = -\frac{aP}{\pi}\left[\frac{\pi \sin^2\alpha}{2\alpha} - 1\right] \qquad \text{(A-7)}$$

Using this expression for M_2 in Equations (A-4b) and (A-5), the complete set of equations for N_ϕ and M_ϕ is written.

$$N_\phi = \frac{P}{2\alpha}\left[\cos\alpha \cos\phi - 1\right]$$

$$M_\phi = aP\left[\frac{1}{\pi} - \frac{1}{2\alpha} + \frac{\cos\alpha\cos\phi}{2\alpha}\right]$$

for $0 \leq \phi \leq \alpha$, and

$$N_\phi = -\frac{P\sin\alpha\sin\phi}{2\alpha}$$

$$M_\phi = aP\left[\frac{1}{\pi} - \frac{\sin\alpha\sin\phi}{2\alpha}\right]$$

for $\alpha \leq \phi \leq \pi/2$. These equations are non-dimensionalized and evaluated for ϕ = 0, 30, 60 and 90 degrees for all three case loads. The results are entered in Table AI.

TABLE A I

ANALYTICAL SOLUTION RESULTS

ϕ		Case 1 Load	Case 2 Load	Case 3 Load
0^o	$\bar{N}_\phi$	0.0	-0.128	-0.238
	$\bar{M}_\phi$	0.318	0.190	0.080
30^o	$\bar{N}_\phi$	-0.250	-0.239	-0.270
	$\bar{M}_\phi$	-0.068	0.080	0.048
60^o	$\bar{N}_\phi$	-0.433	-0.413	-0.358
	$\bar{M}_\phi$	-0.115	-0.095	-0.040
90^o	$\bar{N}_\phi$	-0.500	-0.477	-0.413
	$\bar{M}_\phi$	-0.182	-0.159	-0.095

APPENDIX B

SOLUTION FOR INITIAL FORCES

The techniques used to obtain the initial fixed end moments and forces required for the finite element solutions to Case 2 and Case 3 loads involve superposition and Castigliano's Theorem. Figure B 1 shows the finite element, the three loading conditions, the boundary forces and moments, and the notation used. The superposition of the forces and moments in Figure B 1 (II) and B 1 (III) is equivalent to the forces and moments in Figure B 1 (I). The sum of the rotations of the ends of the element in Figure B 1 (II) and (III) must be zero. Thus, $\theta_{II} + \theta_{III} = 0$. However, since θ_{II} is zero under the end conditions and loading of Figure B 1 (II), $\theta_{III} = 0$. The analogous requirement for the horizontal displacements of the ends of the element of Figure B 1 (II) and (III) leads to

$$\delta_{II} = \delta_{III} \tag{B-1}$$

where δ_{II} is the horizontal component of the known radial displacement of (II), and δ_{III} is the horizontal displacement obtained from an expression for the strain energy of the element in Figure B 1 (III) using Castigliano's Theorem. δ_{II} is positive in the direction towards the centerline, and δ_{III} is positive in the direction away from the centerline.

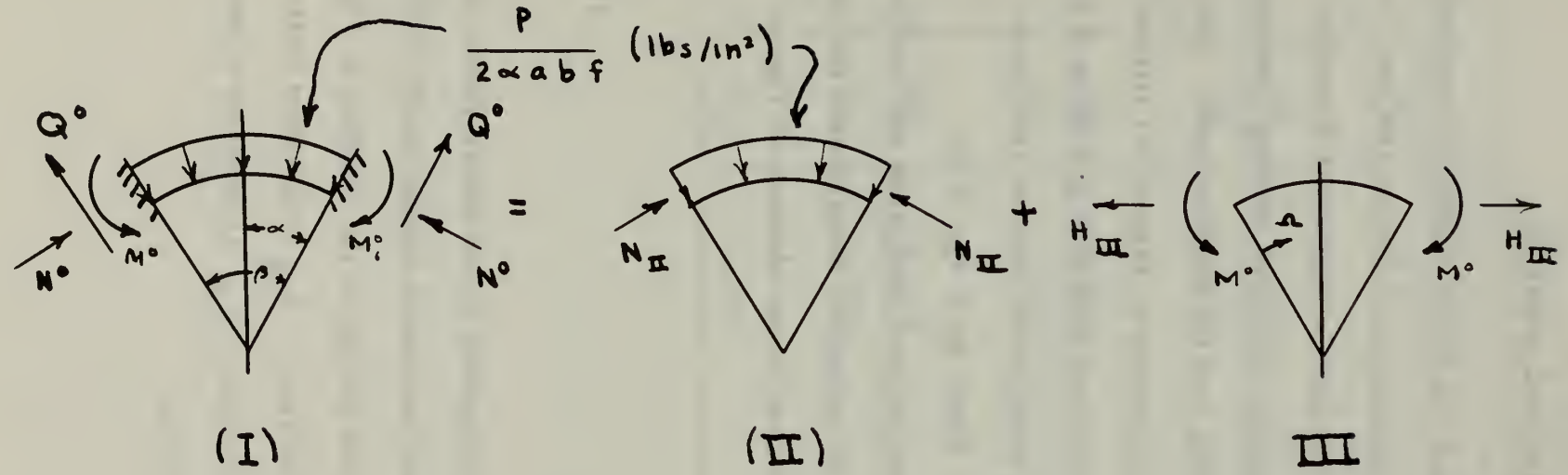

FIGURE B 1

RING SEGMENTS USED IN FIXED END SOLUTION

Letting α be the half angle of the element and ϕ be the angle at any point along the element, the moment at ϕ is

$$M_\phi = M^\circ - aH_{III}\left[\cos\phi - \cos\alpha\right]$$

And the axial force at ϕ is

$$N_\phi = H_{III}\cos\phi$$

The strain energy, U_t from both axial extension and bending of the total element is

$$U_t = 2\int_0^\alpha \frac{M_\phi^2}{2EI}\,a\,d\phi + 2\int_0^\alpha \frac{N_\phi^2}{2AE}\,a\,d\phi \qquad \text{(B-2)}$$

Using Equation (B-2) in Castigliano's Theorem gives

$$2\delta_{III} = \frac{\partial U_t}{\partial H_{III}} \qquad \text{(B-3)}$$

Substituting Equation (B-2) into Equation (B-3), differentiating, integrating and applying limits yield

$$\delta_{III} = \frac{a}{EI}\left[a^2 H_{III}\left(-\frac{1}{\alpha}\left\{\sin\alpha - \alpha\cos\alpha\right\}^2 + \frac{1}{2}\right.\right.$$

$$\left.\left. - \frac{3\sin 2\alpha}{4} + \alpha\cos^2\alpha\right)\right] + \frac{aH_{III}}{AE}\left[\frac{\alpha}{2}\right. \qquad \text{(B-4)}$$

$$\left. + \frac{\sin 2\alpha}{4}\right]$$

The horizontal displacement δ_{II} is

$$\delta_{II} = \frac{a P \sin\alpha}{2\alpha b f t E} \qquad \text{(B-5)}$$

where f is given by

CASE LOAD	2	3
$\beta = 7.5^{\circ}$	f = 8	f = 16
$\beta = 15.0^{\circ}$	f = 4	f = 8
$\beta = 30.0^{\circ}$	f = 2	f = 4

The factor f is required in order to give the proper portion of the total load P over each of the different segment sizes. Substituting Equations (B-4) and (B-5) into (B-1) leads to

$$\frac{a^3}{EI} H_{III}\left[-\frac{1}{\alpha}\left\{\sin\alpha - \alpha\cos\alpha\right\}^2 + \frac{\alpha}{2} - \frac{3\sin 2\alpha}{4} + \alpha\cos^2\alpha\right]$$

$$+\frac{a}{AE} H_{III}\left[\frac{\alpha}{2} + \frac{\sin 2\alpha}{4}\right] = \frac{a P \sin\alpha}{2\alpha b f t E}$$

The above equation can be simplified to give

$$12\left(\frac{a}{t}\right)^2 H_{III}\left[-\frac{1}{\alpha}\left\{\sin\alpha - \alpha\cos\alpha\right\}^2 + \frac{\alpha}{2} - \frac{3\sin 2\alpha}{4}\right.$$

$$\left. + \alpha\cos^2\alpha\right] + H_{III}\left[\frac{\alpha}{2} + \frac{\sin 2\alpha}{4}\right] = \frac{P\sin\alpha}{2\alpha f} \qquad \text{(B-6)}$$

Thus, H_{III} can be determined from Equation (B-6) for a given case load and a specified central angle for the element, β, once t/a is chosen. The requirement to select a specific t/a ratio in order to

solve Equation (B-6) means that the axial strain energy is included in the expression. Failure to include the axial strain energy by making the assumption made in Reference 2 that it can be neglected for curved elements with small t/a ratios leads to gross errors. This is because the assumption made in Reference 2 is not valid for curved elements with distributed loads over large portions of the element.

The equation for the total normal forces N^o acting on the ends of the element shown in Figure B 1 (I) is

$$N^o = N_{III} - H_{III} \cos\alpha$$

or

$$N^o = \frac{p}{2\alpha f} - H_{III} \cos\alpha \qquad \text{(B-7)}$$

since

$$N_{II} = \frac{p}{2\alpha f}$$

The component of H_{III} in the radial direction is the shear force, Q^o, at the ends of the ring element. Thus

$$Q^o = H_{III} \sin\alpha \qquad \text{(B-8)}$$

In order to obtain M^o, Castigliano's Theorem, in conjunction with the requirement $\theta_{III} = 0$, is used to write

$$\frac{\partial U_t}{\partial M^o} = 0$$

where U_t is given by Equation (B-2).

Differentiation and integration of this equation give

$$M^{o} = a H_{III} \left(\frac{\sin\alpha}{\alpha} - \cos\alpha \right) \qquad \text{(B-9)}$$

Experience with Equations (B-6) through (B-9) shows that the axial strain energy must be included if accurate answers are desired for N^{o}, Q^{o} and M^{o}. Thus, $t/a = 1/10$ is chosen, and Equations (B-6) through (B-9) are used to prepare the entires in Table B I for N^{o}, and M^{o} for Case 2 and 3 loads and $\beta = 30$, 15 and 7.5 degrees. In evaluating these equations, trigonometric functions accurate to 5 decimal places do not give accurate answers for N^{o}, Q^{o} and M^{o} for the values of β used in this thesis. Consequently the entries in Table B I are obtained by using trigonometric functions of 10 decimal place accuracy. Solving equations such as (B-6) using 10 decimal places is obviously beyond the capacity of either slide rule or practical hand calculations. Even with an electronic desk calculator, solving such equations is laborious and time consuming.

TABLE B I

FIXED END RESULTS

CASE 2 LOAD

	7.5^{o}	15^{o}	30^{o}
N^{o}	0.00181929P	0.01286764P	0.12707678P
Q^{o}	0.06247015P	0.12402482P	0.22182251P
M^{o}	0.00136328Pa	0.00541780Pa	0.01944670Pa

CASE 3 LOAD

	7.5^{o}	15^{o}	30^{o}
N^{o}	0.00090964P	0.00643382P	0.06353839P
Q^{o}	0.03123508P	0.06201237P	0.11091125P
M^{o}	0.00068164Pa	0.00270890Pa	0.00972335Pa

APPENDIX C

FORTRAN IV PROGRAMS

TABLE C I

DESCRIPTION OF SUBROUTINE "DSIMQ"

PURPOSE

OBTAIN SOLUTION OF A SET OF SIMULTANEOUS LINEAR EQUATIONS, AX=B

USAGE

CALL "DSIMQ" (A, B, N, KS)

DESCRIPTION OF PARAMETERS

A AND B MUST BE REAL*8

A - MATRIX OF COEFFICIENTS STORED COLUMNWISE. THESE ARE DESTROYED IN THE COMPUTATION. THE SIZE OF MATRIX A IS N BY N.

B - VECTORS OF ORIGINAL CONSTANTS (LENGTH N). THESE ARE REPLACED BY FINAL SOLUTION VALUES, VECTOR X.

N - NUMBER OF EQUATIONS AND VARIABLES

KS - OUTPUT DIGIT
0 FOR A NORMAL SOLUTION
1 FOR A SINGULAR SET OF EQUATIONS

REMARKS

MATRIX A MUST BE GENERAL.
IF MATRIX IS SINGULAR, SOLUTION VALUES ARE MEANINGLESS. AN ALTERNATIVE SOLUTION MAY BE OBTAINED BY USING MATRIX INVERSION (MINV) AND MATRIX PRODUCT (GMPRD).

SUBROUTINES AND FUNCTION SUBPROGRAMS REQUIRED

NONE

METHOD

METHOD OF SOLUTION IS BY ELIMINATION USING LARGEST PIVOTAL DIVISOR. EACH STAGE OF ELIMINATION CONSISTS OF INTERCHANGING ROWS WHEN NECESSARY TO AVOID DIVISION BY ZERO OR SMALL ELEMENTS. THE FORWARD SOLUTION TO OBTAIN VARIABLE N IS DONE IN N STAGES. THE BACK SOLUTION FOR THE OTHER VARIABLES IS CALCULATED BY SUCCESSIVE SUBSTITUTIONS. FINAL SOLUTION VALUES ARE DEVELOPED IN VECTOR B, WITH VARIABLE 1 IN B(1), VARIABLE 2 IN B(2). . . . . , VARIABLE N IN B(N). IF NO PIVOT CAN BE FOUND EXCEEDING A TOLERANCE OF 0.0, THE MATRIX IS CONSIDERED SINGULAR AND KS IS SET TO 1. THIS TOLERANCE CAN BE MODIFIED BY REPLACING THE FIRST STATEMENT.

TABLE C II

LIST OF SYMBOLS USED IN SUBROUTINE "RELM"

Computer Coded Name	Definition
DBETA	β , element central angle.
DESM	Element stiffness matrix $[K_\eta]$.
DESM (I, J)	Stiffness influence coefficient in $[K_\eta]$.
DLA	a (corresponding notation in
DLB	b Reference 3).
DLC	c
DLD	d
DLE	e
DBA	A
DBB	B
DBC	C
DBD	D
DBE	E
DBF	F
DBG	G

TABLE CIII

SUBROUTINE "RELM"

```
      SUBROUTINE RELM(DBETA,DESM,DLA,DLB,DLC,DLD,DLE,DBA,
     1DBB,DBC,DBD,DBE,DBF,DBG)
      DOUBLE PRECISION DLA,DLB,DLC,DLD,DLE,DBA,DBB,DBC,DBD,
     1DBE,DBF,DBG
      DOUBLE PRECISION DBETA
      REAL*8 DESM(6,6)
      DLA=DBETA-DSIN(DBETA)
      DLB=DCOS(DBETA)+((DSIN(DBETA))**2)/2.0D0-1.0D0
      DLC=  (3.0D0*DBETA)/2.0D0-2.0D0*DSIN(DBETA)+
     1(DSIN(2.0D0*DBETA))/4.0D0
      DLC=DBETA/2.0D0-(DSIN(2.0D0*DBETA))/4.0D0
      DLE=DCOS(DBETA)-1.0D0
      DBA=(DLE**2)/DBETA-DLD
      DBB=DLB-(DLA*DLE)/DBETA
      DBC=DLA*DLD-DLB*DLE
      DBD=(DLA**2)/DBETA-DLC
      DBE=DLC*DLE-DLA*DLB
      DBF=(DLB**2)-(DLC*DLD)
      DBG=DLB*(DLB-(2.0D0*DLA*DLE)/DBETA)+DLC*
     1(-DLD+((DLE**2)/DBETA))+((DLA**2)*DLD)/DBETA
      DESM(1,1)=DBA/DBG
      DESM(1,2)=DBB/DBG
      DESM(1,3)=DBC/(DBETA*DBG)
      DESM(2,1)=DBB/DBG
      DESM(2,2)=DBD/DBG
      DESM(2,3)=DBE/(DBETA*DBG)
      DESM(3,1)=DBC/(DBETA*DBG)
      DESM(3,2)=DBE/(DBETA*DBG)
      DESM(3,3)=DBF/(DBETA*DBG)
      DESM(4,1)=-(DBA*DCOS(DBETA)+DBB*DSIN(DBETA))/DBG
      DESM(4,2)=-  (DBB*DCOS(DBETA)+DBD*DSIN(DBETA))/DBG
      DESM(4,3)=-   (DBC*DCOS(DBETA)+DBE*DSIN(DBETA))/
     1(DBETA*DBG)
      DESM(5,1)=    (DBA*DSIN(DBETA)-DBB*DCOS(DBETA))/DBG
      DESM(5,2)=   (DBB*DSIN(DBETA)-DBD*DCOS(DBETA))/DBG
      DESM(5,3)=   (DBC*DSIN(DBETA)-DBE*DCOS(DBETA))/
     1(DBETA*DBG)
      DESM(6,1)=     (DBA*(DCOS(DBETA)-1.0D0)+DBB*
     1(DSIN(DBETA))-DBC/DBETA)/DBG
      DESM(6,2)=   (DBB*(DCOS(DBETA)-1.0D0)+DBD*
     1DSIN(DBETA)-DBE/DBETA)/DBG
      DESM(6,3)=   (DBC*(DCOS(DBETA)-1.0D0)+DBE*
     1DSIN(DBETA)-DBF)/(DBETA*DBG)
      DESM(4,4)=DESM(1,1)
      DESM(4,5)=-DESM(1,2)
      DESM(4,6)=DESM(1,3)
      DESM(5,4)=-DESM(2,1)
      DESM(5,5)=DESM(2,2)
      DESM(5,6)=-DESM(2,3)
      DESM(6,4)=DESM(3,1)
      DESM(6,5)=-DESM(3,2)
      DESM(6,6)=DESM(3,3)
      DESM(1,4)=DESM(4,1)
      DESM(1,5)=DESM(5,1)
      DESM(1,6)=DESM(6,1)
      DESM(2,4)=DESM(4,2)
      DESM(2,5)=DESM(5,2)
      DESM(2,6)=DESM(6,2)
      DESM(3,4)=DESM(4,3)
      DESM(3,5)=DESM(5,3)
      DESM(3,6)=DESM(6,3)
      RETURN
      END
```

TABLE C IV

LIST OF SYMBOLS USED IN

PROGRAM "BETA 30"

Computer Coded Name	Definition
A	Reduced stiffness matrix $[K_\rho]$.
A (I, J)	Stiffness influence coefficient in $[K_\rho]$.
B (I)	Prior to calling "DSIMQ" B(I) = $\{\{X\} - \{X^0\}\}$.
B (I)	After calling "DSIMQ" B (I) = $\{u_\rho\}$.
DBETA	β , element central angle.
DESM	Element stiffness matrix $[K_\eta]$.
DESM (I, J)	Stiffness influence coefficient in $[K_\eta]$.
PI	π
DM (I)	Moment at node (I).
DN (I)	Normal force at node (I).

TABLE CV

PROGRAM "BETA30"

```
C   PROGRAM BETA 30
        DOUBLE PRECISION DBETA,PI,DLA,DLB,DLC,DLD,DLE,DBA,
       1DBB,DBC,DBD,DBE,DBF,DBG
     91 FORMAT (1HO,1P6D20.10)
     92 FORMAT (1HO,1P5D19.10)
     93 FORMAT (1HO,1P7D18.10)
     94 FORMAT (1HO,1PD20.10)
     11 FORMAT (1HO,1P5D20.10)
     12 FORMAT (1HO,1PD20.10)
     13 FORMAT (1HO,1P6D20.10)
     14 FORMAT (1HO,1P9D15.7)
     15 FORMAT (1H1,'DISPLACEMENTS')
     16 FORMAT (1HO,'FORCES AND MOMENTS')
     17 FORMAT (1HO,'CASE 2 BETA=30 DEGREES')
     22 FORMAT(1HO,1PD20.10)
     23 FORMAT(I2)
     24 FORMAT(1HO,1PD20.10)
        PI=3.14159265358979300
        DBETA=PI/6.0D0
        WRITE (6,94) DBETA
        REAL*8 DESM(6,6)
        CALL RELM (DBETA,DESM,DLA,DLB,DLC,DLD,DLE,DBA,
       1DBB,DBC,DBD,DBE,DBF,DBG)
        WRITE (6,92) DLA,DLB,DLC,DLD,DLE
        WRITE (6,93)DBA,DBB,DBC,DBD,DBE,DBF,DBG
        WRITE (6,91) ((DESM(I,J),J=1,6),I=1,6)
C FORBETA=30DEGREES
        REAL*8A(8,8)
        DO 110 I=1,8
        DO 111 J=1,8
        A(I,J)=0.0D0
   111 CONTINUE
   110 CONTINUE
        A(1,1)=DESM(2,2)
        A(2,1)=DESM(4,2)
        A(3,1)=DESM(5,2)
        A(4,1)=DESM(6,2)
        A(1,2)=DESM(2,4)
        A(2,2)=DESM(4,4)+DESM(1,1)
        A(3,2)=DESM(5,4)+DESM(2,1)
        A(4,2)=DESM(6,4)+DESM(3,1)
        A(5,2)=DESM(4,1)
        A(6,2)=DESM(5,1)
        A(7,2)=DESM(6,1)
        A(1,3)=DESM(2,5)
        A(2,3)=DESM(4,5)+DESM(1,2)
        A(3,3)=DESM(5,5)+DESM(2,2)
        A(4,3)=DESM(6,5)+DESM(3,2)
        A(5,3)=DESM(4,2)
        A(6,3)=DESM(5,2)
        A(7,3)=DESM(6,2)
        A(1,4)=DESM(2,6)
        A(2,4)=DESM(4,6)+DESM(1,3)
        A(3,4)=DESM(5,6)+DESM(2,3)
        A(4,4)=DESM(6,6)+DESM(3,3)
        A(5,4)=DESM(4,3)
        A(6,4)=DESM(5,3)
        A(7,4)=DESM(6,3)
        A(2,5)=DESM(1,4)
        A(3,5)=DESM(2,4)
        A(4,5)=DESM(3,4)
        A(5,5)=DESM(4,4)+DESM(1,1)
        A(6,5)=DESM(5,4)+DESM(2,1)
        A(7,5)=DESM(6,4)+DESM(3,1)
        A(8,5)=DESM(5,1)
```

```
      A(2,6)=DESM(1,5)
      A(3,6)=DESM(2,5)
      A(4,6)=DESM(3,5)
      A(5,6)=DESM(4,5)+DESM(1,2)
      A(6,6)=DESM(5,5)+DESM(2,2)
      A(7,6)=DESM(6,5)+DESM(3,2)
      A(8,6)=DESM(5,2)
      A(2,7)=DESM(1,6)
      A(3,7)=DESM(2,6)
      A(4,7)=DESM(3,6)
      A(5,7)=DESM(4,6)+DESM(1,3)
      A(6,7)=DESM(5,6)+DESM(2,3)
      A(7,7)=DESM(6,6)+DESM(3,3)
      A(8,7)=DESM(5,3)
      A(5,8)=DESM(1,5)
      A(6,8)=DESM(2,5)
      A(7,8)=DESM(3,5)
      A(8,8)=DESM(5,5)
   21 FORMAT(1HO,1P8D16.8)
      WRITE(6,21) ((A(I,J),J=1,8),I=1,8)
      REAL*4 R(8,8)
      DO 301 I=1,8
      DO 302 J=1,8
      R(I,J)=A(I,J)
  302 CONTINUE
  301 CONTINUE
      REAL*8B(8)
      DO 112 I=1,8
      B(I)=0.0D0
  112 CONTINUE
C B LOAD MATRIX FOR CASE 2. BETA=30 DEG.
      B(1)=.22182251D0
      B(2)=.12707678D0
      B(3)=.22182251D0
      B(4)=-.01944670D0
      WRITE(6,22) (B(I),I=1,8)
      N=8
      CALL DSIMQ (A,B,N,KS)
      WRITE(6,23) (KS)
      WRITE (6,12)  (B(I),I=1,8)
      WRITE (6,15)
      WRITE (6,12) B(1)
      WRITE (6,12) B(3)
      WRITE (6,12) B(6)
      WRITE (6,12) B(8)
      DOUBLE PRECISION DN1,DQ1,DM1,DN2,DQ2,DM2,
     1DN3,DQ3,DM3,DN4,DQ4,DM4
C FORCES AND MOMENTS FOR CASE 2. BETA=30 DEGREES
      DN1=DESM(1,2)* B(1)+DESM(1,4)*B(2)+DESM(1,5)* B(3)
     1+DESM(1,6)*B(4)+.12707678D0
      DM1=DESM(3,2)* B(1) +DESM(3,4)*B(2)+DESM(3,5)*
     1B(3)+DESM(3,6)*B(4)-.01944670D0
      DN2=DESM(4,2)* B(1) +DESM(4,4)*B(2)+DESM(4,5)*
     1B(3)+DESM(4,6)*B(4)-.12707678D0
      DM2=DESM(6,2) * B(1) +DESM(6,4)*B(2)+DESM(6,5)*
     1B(3)+DESM(6,6)*B(4)+.01944670D0
      DN3=DESM(1,1)*B(5)+DESM(1,2)* B(6)+DESM(1,3)*B(7)
     1+DESM(1,5)*B(8)
      DM3=DESM(3,1)*B(5)+DESM(3,2)* B(6) +DESM(3,3)
     1*B(7)+DESM(3,5)*B(8)
      DN4=DESM(4,1)*B(5)+DESM(4,2)* B(6) +DESM(4,3)
     1*B(7)+DESM(4,5)*B(8)
      DM4=DESM(6,1)*B(5)+DESM(6,2)*B(6)+DESM(6,3)*B(7)
     1+DESM(6,5)*B(8)
      WRITE (6,17)
      WRITE (6,16)
      WRITE (6,12) DN1,DM1,DN2,DM2,DN3,DM3,DN4,DM4
      STOP
      END
```

INITIAL DISTRIBUTION LIST

		No. Copies
1.	Defense Documentation Center Cameron Station Alexandria, Virginia 22314	20
2.	Library Naval Postgraduate School Monterey, California 93940	2
3.	Commander, Naval Air Systems Command Navy Department Washington, D. C. 20360	1
4.	Commandant of the Marine Corps (Code AO3C) Headquarters, U. S. Marine Corps Washington, D. C. 20380	1
5.	Professor Robert E. Ball Department of Aeronautics Naval Postgraduate School Monterey, California 93940	5
6.	Professor Charles H. Kahr Department of Aeronautics Naval Postgraduate School Monterey, California 93940	1
7.	Chairman, Department of Aeronautics Naval Postgraduate School Monterey, California 93940	1
8.	Professor A. E. Fuhs Department of Aeronautics Naval Postgraduate School Monterey, California 93940	1
9.	Major Owen C. Baker, USMC P. O. Box 4643 Carmel, California 93921	2
10.	Dr. F. I. Tanczos AIR (03B) Technical Director Research and Technology Naval Air Systems Command Washington, D. C. 20360	1
11.	Commandant of the Marine Corps (MC-AX-2) Attn: Dr. Alexander L. Slafkosky Headquarters, U. S. Marine Corps Washington, D. C. 20380	1

12. Dr. E. S. Lamar (Code 03C) — 1
Chief Scientist
Naval Air Systems Command
Washington, D. C. 20360

13. Dr. R. S. Burington — 1
Chief Mathematician
Naval Air Systems Command
Washington, D. C. 20360

14. Commander — 1
Naval Ordnance Systems Command
Washington, D. C. 20360

15. Mr. G. L. Desmond — 1
Aerodynamics and Structures Admin. (Code 320)
Research and Technology
Naval Air Systems Command
Washington, D. C. 20360

16. Mr. R. E. Davison — 1
Equipment and Support Administrator (Code 340)
Research and Technology
Naval Air Systems Command
Washington, D. C. 20360

17. Office of Naval Research — 1
Physical Sciences Division, Code 420
Washington, D. C. 20360

18. Office of Naval Research — 1
(Attn: R. D. Cooper, Code 438)
Material Sciences Division
Office of Naval Research
Washington, D. C. 20360

19. Office of Naval Research — 1
Mathematical Sciences Division, Code 430
Washington, D. C. 20360

20. Office of Naval Research — 1
Air Programs Office
Washington, D. C. 20360

UNCLASSIFIED

DOCUMENT CONTROL DATA - R & D

Security classification of title, body of abstract and indexing annotation must be entered when the overall report is classified)

ORIGINATING ACTIVITY (Corporate author)
Naval Postgraduate School,
Monterey, California 93940

2a. REPORT SECURITY CLASSIFICATION
Unclassified

2b. GROUP

REPORT TITLE
A Comparison of Finite Element and Fourier Series Solutions as Applied to Radially Loaded Circular Rings

DESCRIPTIVE NOTES (Type of report and inclusive dates)
Thesis

AUTHOR(S) (First name, middle initial, last name)
Owen C. Baker

REPORT DATE	7a. TOTAL NO. OF PAGES	7b. NO. OF REFS
June 1968	77	5

8a. CONTRACT OR GRANT NO.

b. PROJECT NO

c.

d.

9a. ORIGINATOR'S REPORT NUMBER(S)

9b. OTHER REPORT NO(S) (Any other numbers that may be assigned this report)

10 DISTRIBUTION STATEMENT
[redacted]

11. SUPPLEMENTARY NOTES

12. SPONSORING MILITARY ACTIVITY
Naval Postgraduate School,
Monterey, California 93940

13 ABSTRACT

An examination and a comparison of the relative merits of the finite element and Fourier series methods of solving radially loaded circular ring problems are made. The procedure employed to evaluate the two methods is to use each method to solve for three different load conditions and to compare the performance of the two methods on the basis of accuracy, ease of usage, and equipment required. The results indicate a satisfactory accuracy for both methods under most conditions. The Fourier series method is superior for solving problems with a distributed load condition. The finite element method is superior for solving multiple problems with concentrated loads.

DD FORM 1 NOV 65 1473 (PAGE 1)
S/N 0101-807-6811

A-31408

UNCLASSIFIED

14 KEY WORDS	LINK A		LINK B		LINK C	
	ROLE	WT	ROLE	WT	ROLE	WT
FINITE ELEMENT						
FOURIER SERIES						
CIRCULAR RINGS						

[redacted]